Probabilistic seismic hazard analysis model for the Philippines

Henremagne C Peñarubia[1], Kendra L Johnson[2], Richard H Styron[2], Teresito C Bacolcol[1], Winchelle Ian G Sevilla[1], Jeffrey S Perez[1], Jun D Bonita[1], Ishmael C Narag[1], Renato U Solidum Jr[1], Marco M Pagani[2] and Trevor I Allen[3] [iD]

Abstract

The Philippine archipelago is tectonically complex and seismically hazardous, yet few seismic hazard assessments have provided national coverage. This article presents an updated probabilistic seismic hazard analysis for the nation. Active shallow crustal seismicity is modeled by faults and gridded point sources accounting for spatially variable occurrence rates. Subduction interfaces are modeled with faults of complex geometry. Intraslab seismicity is modeled by ruptures confined to the slab volume. Source geometries and earthquake rates are derived from seismicity catalogs, geophysical data sets, and historic-to-paleoseismic constraints on fault slip rates. The ground motion characterization includes models designed for global use, with partial constraint by residual analysis. Shallow crustal faulting near metropolitan Manila, Davao, and Cebu dominates shaking hazard. In a few places, peak ground acceleration with 10% probability of exceedance in 50 years on rock reaches 1.0*g*. The results of this study may have utility for defining the design base shear in the National Structural Code of the Philippines.

Keywords

Acceleration maps, design standards, earthquake hazard analysis, probabilistic seismic hazard analysis, Philippines

[1]Philippine Institute of Volcanology and Seismology - Department of Science and Technology, Philippines (PHIVOLCS-DOST Philippines)
[2]Global Earthquake Model (GEM) Foundation, Pavia, Italy
[3]Geoscience Australia, Canberra, ACT, Australia

Corresponding author:
Kendra L Johnson, Global Earthquake Model (GEM) Foundation, Via Ferrata 1, 27100 Pavia, Italy.
Email: kendra.johnson@globalquakemodel.org

Introduction

The Philippines sits in a complex tectonic environment characterized by rapid relative plate motion, high slip rates, and consequent high seismic hazard. Despite this situation, there have been few probabilistic seismic hazard analysis (PSHA) studies published on a national scale (Molas and Yamazaki, 1994; Su, 1988; Thenhaus et al., 1994; Torregosa et al., 2002). In the latest version of the National Structural Code of the Philippines (NSCP, 2015), a referral code of the National Building Code, the seismic coefficient—a factor that indicates the expected force of earthquake shaking used to calculate the seismic design base shear of structures—ranges from 0.16g to 0.66g depending on the soil classification, source-site distance, and type of seismic source. However, recent destructive events in the Philippines such as the 6 February 2012 M_S 6.9 Negros Oriental Earthquake, the 15 October 2013 M_S 7.2 Bohol Earthquake, and the 10 February 2017 M_S 6.7 offshore Surigao Earthquake significantly exceeded the prescribed seismic coefficients set by the NSCP (Peñarubia, 2017).

The Philippine Institute of Volcanology and Seismology (PHIVOLCS) of the Department of Science and Technology (DOST) is a service institute of the Philippine government principally mandated to mitigate disasters that may arise from volcanic eruptions, earthquakes, tsunami, and other related geophysical phenomena. In response to the 2013 and 2017 earthquakes, PHIVOLCS initiated a probabilistic seismic hazard study (Peñarubia et al., 2017) using a similar approach to Thenhaus et al. (1994), but with updated seismicity and source-zone geometry, and more modern ground motion models (GMMs). The results were presented for approval to the national and local stakeholders including government agencies, the structural engineering community, insurance and business sector, city and municipal government units, and academe. In the series of meetings and considerations, the model was modified by consensus, finalized, and launched in a press conference as the Philippine Earthquake Model (PEM) Atlas in January 2018. That model was intended for direct use in the seismic design of structures in the Philippines. However, some technical experts have been cautious to accept the significant changes and design impact through this development, hence prompting the need for validation and international collaboration. Here, an updated and more detailed seismic hazard model for the Philippines is presented, developed in a collaboration between PHIVOLCS and the Global Earthquake Model (GEM) Foundation. The model will be made openly available through the GEM Global Hazard Mosaic.

Tectonic setting and regionalization

The Philippine archipelago is a group of crustal blocks wedged between the Philippine Sea Plate to the east and the Sunda Plate to the west. These two plates are being consumed by active subduction zones on both sides of the archipelago. Because of these double-divergent subduction zones, the overall tectonics of this region and the resulting active structures are generally considered to be some of the most complex on Earth (Yumul et al., 2003; Figure 1).

In Luzon, the northernmost major island in the Philippines, the majority of plate convergence between the Sunda and Philippine Sea plates occurs on the east-dipping Manila Trench, which extends from ~12 to 23°N. Its slip convergence decreases from ~90 mm/year in the north to ~60 mm/year in the south (Hsu et al., 2016). At these latitudes, some of the plate convergence may also be partitioned along the East Luzon Trough, which dips westward beneath eastern Luzon and may be structurally continuous north to Taiwan. East of Luzon Island, a slip rate of about 10 mm/year has been inferred from geodetic
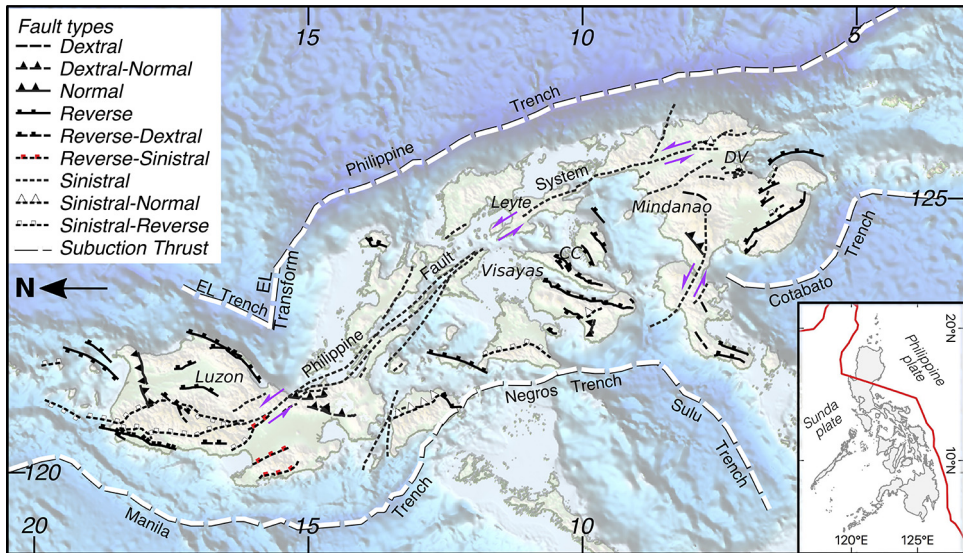
Figure 1. Overview of tectonic structures. Dashed white lines show the subduction trenches. Thin lines are active crustal faults patterned by sense of motion. Active faults and trenches are according to the PHIVOLCS database as of July 2018. Inset shows the Philippines relative to main tectonic plates. EL: East Luzon; MM: Metro Manila; CC: Metro Cebu; DV: Metro Davao.

measurements (e.g. Galgana et al., 2007; Hsu et al., 2016). A transform fault connects the East Luzon Trough to the Philippine Trench. The Philippine Trench absorbs the subduction of the Philippine Sea Plate at about 30 mm/year (Galgana et al., 2007) and continues toward the south until Mindanao. In contrast, the Manila Trench on the west terminates where the bathymetrically high Palawan Block collides with the Philippines (Yumul et al., 2005). The east-dipping subduction resumes farther south along the Negros Trench.

The subduction configuration in the southern Philippines is more complex and less constrained than in the north. From Panay to the southwestern-most Philippine islands, the Sulu oceanic basin subducts along the east-dipping Negros–Sulu trench system (~26–44 mm/year convergence; e.g. Rangin, 2016), while the Celebes oceanic basin subducts at the Cotabato Trench at ~35 mm/year convergence (Rangin et al., 1999). South of this archipelago, the Molucca Sea floor is deformed by thrust faults that originated during the double-divergent subduction of the Molucca Sea plate. This region, and the fully subducted bi-directionally dipping Halmahera slab, is highly seismically productive today (Zhang et al., 2017).

The Philippine archipelago is actively deforming and transected throughout by active faults (Figure 1). The source of the most destructive earthquakes in the Philippines is the 1250-km-long left-lateral Philippine Fault System (PFS). This fault system partly absorbs the oblique convergence (Fitch, 1972) of motion between the Sunda Plate and Philippine Sea Plate by about 20–25 mm/year (Barrier et al., 1991). However, the PFS is multistranded and segmented through much of its length, and individual strands may have much lower slip rates as revealed by GPS measurements (Aurelio, 2000; Bacolcol, 2003; Bacolcol et al., 2005, 2017; Galgana et al., 2007; Hsu et al., 2016; Yu et al., 1999) and paleoseismic studies (Daligdig, 1997; Papiona and Kinugasa, 2008; Perez et al., 2015; Perez and Tsutsumi, 2011, 2017; Tsutsumi and Perez, 2013; Tsutsumi et al., 2006, 2015).

In central Luzon, the NW-striking Digdig Fault is the principal strand, accommodating most of the slip on the system; this fault hosted the 1990 M_w 7.8 earthquake (e.g. Daligdig, 1997; Nakata et al., 1996). To the north, the PFS changes to a north strike and bifurcates into several branches that bound the Northern Cordillera, causing an increase in contraction, a decrease in the translation rates across the fault (e.g. Galgana et al., 2007; Hsu et al., 2016), and perhaps continued uplift of the Northern Cordillera. The net slip rates on these reverse-sinistral and thrust faults are from ~3.5 to ~17 mm/year (Galgana et al., 2007; Hsu et al., 2016). The multi-stranded nature of these faults, and the increased down-dip width of the dipping faults as compared to vertical strike-slip faults, raises the potential for large earthquakes and high ground shaking over a wider region than elsewhere along the PFS.

Active shallow crustal faulting away from the PFS and distributed throughout the archipelago accommodates deformation for which the PFS and subduction zones are not optimally oriented. This faulting is less studied and more tectonically varied. Northwestern Mindanao hosts normal faults (e.g. Pubellier et al., 1999), while focal mechanisms from the Visayas indicate distributed NE-striking reverse faults bounding these islands.

Because of the complexity of its tectonic setting, estimating the rates and describing the mechanisms and distribution of active faults in the Philippines remains a challenge. However, as the quantity and quality of data increase, particularly through geodetic and paleoseismic studies, the sources of earthquake hazard in the Philippines are becoming better understood.

Earthquake catalog

The earthquake catalog used to produce and test the Philippines hazard source model is a merged version of the ISC-GEM extended catalog (Weatherill et al., 2016) and the PHIVOLCS catalog, a part of the Philippine Earthquake Model Probabilistic Seismic Hazard Analysis Database (see http://www.phivolcs.dost.gov.ph; Bautista and Oike, 2000; Garcia et al., 1985; Thenhaus et al., 1994). The catalogs were merged by stacking the two catalogs, and then purging duplicate events. The ISC-GEM event information is used in cases of duplicates, because the catalog is more extensive, and the consistency is important in catalog preprocessing steps. The resulting catalog has ~37,000 earthquakes, ~160 of which are contributed by the PHIVOLCS catalog, and ranges from 1619 to 2015, including 15 earthquakes $M_w > 7.0$ that predate the 1905 start of the ISC-GEM catalog. While the PHIVOLCS contribution includes both historical and instrumental earthquakes, the ISC-GEM catalog is exclusively instrumental, including some earthquakes as small as M_w 2.8, but the completeness magnitude varies with time. Here, earthquakes with $M_w < 5.0$ are used to help define source geometry, but not to compute seismicity rates.

Prior to developing the seismic source model, the earthquake catalog was pre-processed to prepare sub-catalogs of independent (mainshock) earthquakes that correspond to each tectonic region, including tectonic classification of earthquake hypocenters, catalog declustering, and filtering for completeness, each described in more detail below.

Tectonic classification

The classification of seismicity into the main tectonic contexts (e.g. interface, intraslab, and crustal) is fundamental to constructing the seismic source model for a complex tectonic environment like the Philippines. The routine used here assigns a main tectonic context to
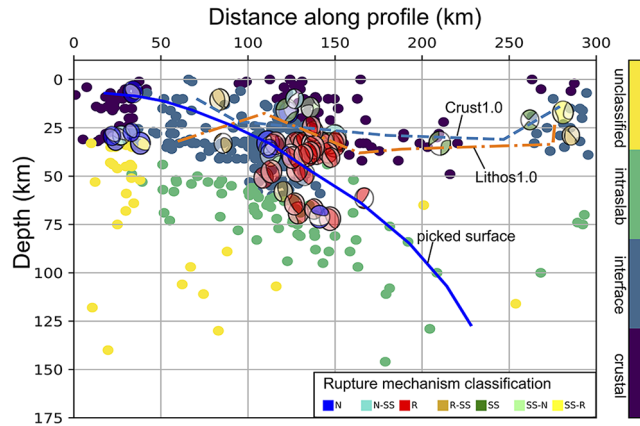
Figure 2. Example cross section with classified earthquakes. Dashed lines are Moho estimates from Crust1.0 and Litho1.0; the Crust1.0 depth to Moho is used as a reference frame for crustal assignment. Solid blue line is the picked surface indicating the subduction interface and slab top. Hypocenters are colored by classification. Subduction earthquakes at distances >250 km correspond to the Philippine Trench. Focal mechanisms are colored by Kaverina classification (Kaverina et al., 1996). Profile location is shown in Figure 3b.

each earthquake in the ISC-GEM/PHIVOLCS-merged catalog based on the proximity of the hypocenter to the Moho, the subduction interface, and the slab top (the top surface of the subducting slab, but deeper than the interface locking depth), each with a depth buffer, categorizing each as crustal, interface, or intraslab; earthquakes that do not comply with any tectonic context are labeled unclassified. Subduction interface and slab sources are further subdivided into segments, permitting the computed seismicity rates to vary along strike. The classification of large earthquakes ($M_w > 7.0$) is manually confirmed, and earthquakes suspected to be incorrectly classified—such as those with default depths that bias the automated routine—are manually reassigned.

The subduction interface and slab top surfaces are defined through a manual examination of the subduction zone structure and earthquake distribution. The details of this process and the remaining tectonic classification steps—including the choices of depth limits and trench segmentation—are described in Supplemental Appendix A.

The Philippines seismic source model includes the Manila, East Luzon, Philippine, Negros, Sulu, and Cotabato trenches, and the fully submerged Halmahera slab. Despite being a transform fault, the East Luzon transform is included, since Slab 2.0 (Hayes et al., 2018) models this surface, and its seismicity rates are high enough to compute a Gutenberg–Richter (GR) magnitude-frequency distribution (MFD), (Gutenberg and Richter, 1944). The surface projections of the subduction interfaces and slab tops used to build the source model, and the classified seismicity, are shown in Figure 3b. Classified hypocenters about the subduction interface and slab top for one cross section through the Manila Trench are shown in Figure 2.

Declustering

Classical PSHA theory requires earthquake sources follow a Poisson process in that each event is independent in space and time (e.g. Gardner and Knopoff, 1974). In the context

of earthquake catalogs, main shocks occur on a space- and time-independent basis over broad regions with similar seismotectonic characteristics (e.g. Gardner and Knopoff, 1974; Musson, 1999). Consequently, it is necessary to remove, or "decluster," dependent events from the earthquake catalog (i.e. fore- and aftershocks). Here, the classified catalogs were declustered following Gardner and Knopoff (1974) using the Uhrhammer (1986) windows. In total, the classified catalogs include ~25,000 mainshocks, of which 14% are interface, 51% are intraslab, and 35% are shallow crustal.

Because seismicity interacts among adjacent tectonic contexts (i.e. interface mainshocks can trigger crustal aftershocks), several domains were declustered together, and then the earthquakes were separated into classified, declustered sub-catalogs. The two declustering groups were crustal, interface, and shallow slab seismicity (which lies laterally beneath the interface) and deep slab. The declustering algorithm works in two spatial dimensions, comparing epicenters and not hypocenters. Thus, for steep subduction geometry, where much of the deep slab would occupy the triggering window for large interface or crustal earthquakes, this distinction between the two groups is critical.

Seismic source characterization

Herein, the characterization of seismicity and construction of a source model for the Philippines is described. The source model includes shallow crustal and subduction zone (i.e. interface and intraslab) seismicity and consists of a single logic tree branch, in which each described source is given full weight. The source geometries are modeled by points, faults with both simple and complex geometry, and predefined ruptures. Rates are derived from a combination of observed earthquake occurrence rates and tectonics.

Active shallow faults

The Philippines shallow fault sources are based on a data set with 115 faults distributed throughout the archipelago. The fault traces are taken from the previous PHIVOLCS compilation used in the PEM model (Peñarubia, 2017; as shown here: https://www.phivolcs.dost.gov.ph%20index.php/earthquake/earthquake-generators-of-the-philippines, last accessed January 2020), with minor updates for fault kinematics and slip rate estimates (1–28 mm/year) based on a synthesis of GPS and paleoseismic studies, with expert judgment considering the total crustal strain budget and seismic history where no precise information exists.

The crustal faults sources were implemented using the Fault Modeler tool in the OpenQuake Model Building Toolkit (https://github.com/GEMScienceTools/oq-mbtk). All faults in the fault database were transformed into seismic hazard sources using estimates of fault area and slip rate. In most cases, each individual fault is converted into an independent source. The exceptions are cases where continuous or semi-continuous fault segments have identical kinematics and very close slip rates; in these cases, the consecutive traces are linked together into one fault. This step is crucial to producing fault sources large enough—based on magnitude scaling relations—to generate earthquakes of historical and instrumental magnitudes. Furthermore, recent earthquakes, such as the 2016 M_w 7.8 Kaikōura earthquake (e.g. Hamling et al., 2017) and 2010 M_w 7.2 El Mayor Cucapah earthquake (e.g. Fletcher et al., 2014), have demonstrated that within zones of numerous faults and fault segments, earthquakes of larger magnitudes may rupture multiple structures together.

The fault geometry is defined by projecting the surface traces of the faults down to 20 km depth, the assumed brittle–ductile transition depth, according to their assigned dip values. Then, MFDs were created for each fault source based on these criteria: (1) All sources were given a minimum magnitude of 6.5, and a maximum magnitude calculated as a function of the area of the fault using the Leonard (2010) area-to-magnitude scaling relationship (also used to generate ruptures during PSHA calculations), on the principle that the maximum magnitude of the MFD is a full-fault rupture. Faults with a $M_{max} < 6.5$ are incorporated into the distributed seismicity sources. (2) Faults with maximum magnitudes greater than 7.0 are given Youngs and Coppersmith (1985) characteristic MFDs using the computed M_{max} as the center of the boxcar, and all others are given double-truncated GR MFDs where M_{max} is the highest magnitude considered. (3) The b value for each fault is taken from the tectonic region that it inhabits (source zones are described next). (4) The total moment release rate is taken as the product of fault slip rate, fault plane area, assumed crustal shear modulus (32 GPa, a typical value for crustal rocks, e.g. Turcotte and Schubert, 2014), and a coefficient that represents the total component of shear stress accumulation that is released seismically; this value is taken as 0.7 based on calibrations of the complete fault data set with catalog seismicity, and the remaining stress is assumed to be released aseismically (e.g. through creep). (5) For faults with GR MFDs, the a value is chosen so that the total moment release rate integrated over the MFD matches the moment release rate calculated in the previous step. The initial and derived fault source parameters are summarized in Table A1 of Supplemental Appendix C.

Criterion 2 was chosen after testing the different MFD options for fault sources. When double-truncated GR MFDs were used to represent the occurrence rates for all faults, earthquakes of M_w 6.5 were overpredicted compared to the observed rates, while larger magnitudes were underpredicted (see Supplemental Appendix E).

Distributed seismicity

Crustal earthquakes that are not distinctly attributable to a fault source are accounted for as distributed seismicity. To model this, seismicity with common tectonic characteristics is grouped together, and point sources are defined to reflect these characteristics as well as the observed distribution of occurrences.

The modeling approach used here builds on the traditional area source approach to compute representative MFDs. In a following phase, the MFD is distributed across a grid of point sources that represents in a discrete form the seismicity within the source zone. The criteria used to distribute the seismicity are based on spatially varying weights computed using an approach similar to the one used to smooth the seismicity (e.g. Frankel, 1995). The declustered subcatalog of crustal seismicity, filtered for completeness (time-magnitude thresholds in Table 2), is further subdivided into source zones of internally consistent tectonics or geophysical contexts (e.g. outer rise seismicity, fore- and/or backarc thrusting, containing up to a few prominent focal mechanisms), the GR b value is resolved, and then the occurring seismicity is smoothed onto a 0.1° grid of points. This approach allows for larger source zones (and thus more earthquakes to compute a robust MFDs) while still capturing spatial variability in seismicity rate (e.g. Rong et al., 2017).

Each source zone is assigned a double-truncated GR MFD from $M_w = 5$ to $M_{max,obs} + 0.5$ (bins of M_w 0.1 and ruptures scaled using the magnitude scaling relationship of Wells and Coppersmith (1994)), solving for a and b values based on the regression method of Weichert (1980). A probability weighting is assigned to depth bins, and up to a
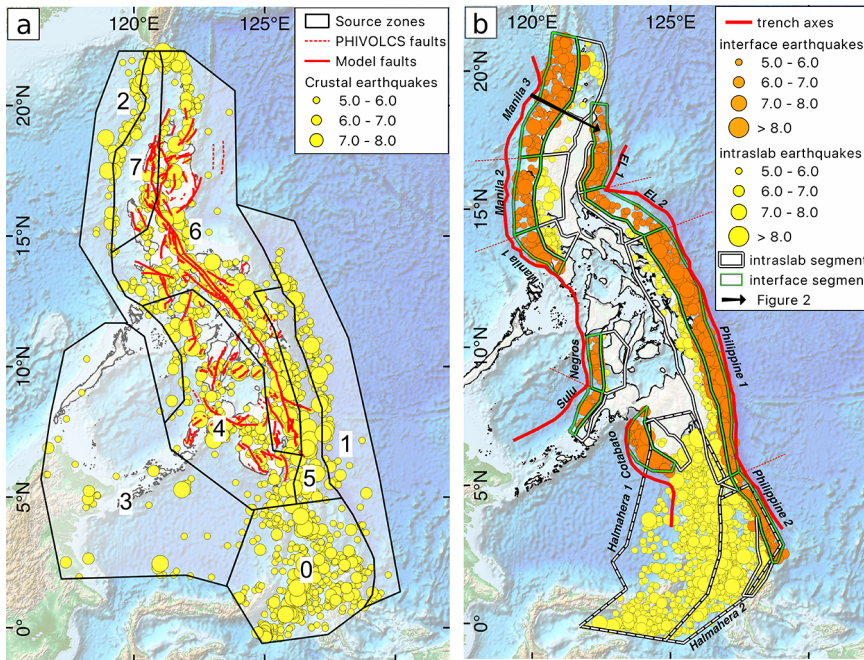
Figure 3. (a) Crustal sources. All catalog earthquakes $M_w > 5.0$ classified as crustal and within the source-zone polygons are included. Red lines are the surface traces of mapped faults, as indicated in the PHIVOLCS fault database as of July 2018. Solid lines show fault traces used to define fault source geometry. Dashed lines are other faults not included in this model. (b) Subduction interface and intraslab source surface projections, with classified seismicity. Green perimeters show the surface projection of the interface segments, and white perimeters show the surface projection of the slab segments (the Halmahera slab is dashed white to help visually distinguish it where slabs are overlapping). Red lines show trench axes originally used to create the cross sections and depth profiles. Seismicity of $M_w > 5$ is colored by tectonic region, where yellow is intraslab and orange in interface, and scaled by magnitude. The black arrow shows coordinates of the cross section in Figure 2, with the arrow pointing in the direction of increasing distance.
EL: East Luzon.

few most-likely nodal planes that are based on crustal events in the Global Centroid Moment Tensor (GCMT) catalog (Ekström et al., 2012). The MFD for the source zone is then smoothed across the seismicity grid by applying a multiple-smoothing Gaussian filter (95% using filter parameters of radius = 50 km and standard deviation = 20 km, and 5% with radius = 20 km and standard deviation = 5 km).

In areas that overlap the fault sources, double counting is prevented by dividing the magnitude occurrence bins between the two source types. If there is overlap with the surface projection of a fault (including a buffer of 15 km), the MFDs for distributed seismicity are truncated at $M_{max} = 6.5$; the fault MFDs use $M_{min} = 6.5$.

The Philippines seismic source characterization uses eight source zones, labeled in Figure 3a. The zone characteristics and MFD parameters are listed in Table 1. Figures 4a and b shows the final MFDs for source zones 4 and 6: two source zones containing faults.

Table 1. Model parameters for crustal source zones

Zone	Description	a	b	$M_{\text{max,obs}}$	N
0	Shallow thrust faulting above the Halmahera slab	5.619	0.959	7.75[a]	251
1	Normal faulting in the Philippine Trench outer rise	4.059	0.796	7.76[a]	48
2	Normal faulting in the Manila, Sulu, and Negros trenches outer rises	5.135	1.019	7.60[a]	42
3	Diffuse crustal seismicity with no predominant mechanism	3.779	0.814	7.15[a]	20
4	Crustal faulting within the southwest archipelago, mostly reverse and left-lateral sense of motion	4.998	0.904	7.80[a]	117
5	Fore- and backarc thrusting in the overriding plate of the Philippine Trench	3.205	0.620	7.69[a]	53
6	High-rate active crustal deformation, dominated by the PFS and associated structures	5.826	1.003	8.00[b]	248
7	Region of mostly normal faulting along the fore-arc of the Manila Trench	5.191	1.098	7.30[a]	19

PFS: Philippine Fault System.

N: number of earthquakes, after declustering and filtering for completeness. a and b: zonal a and b values.

[a]The largest recorded earthquake was pre-1964 and could have a high magnitude error or was filtered out using the completeness thresholds and thus not used to compute the MFD.
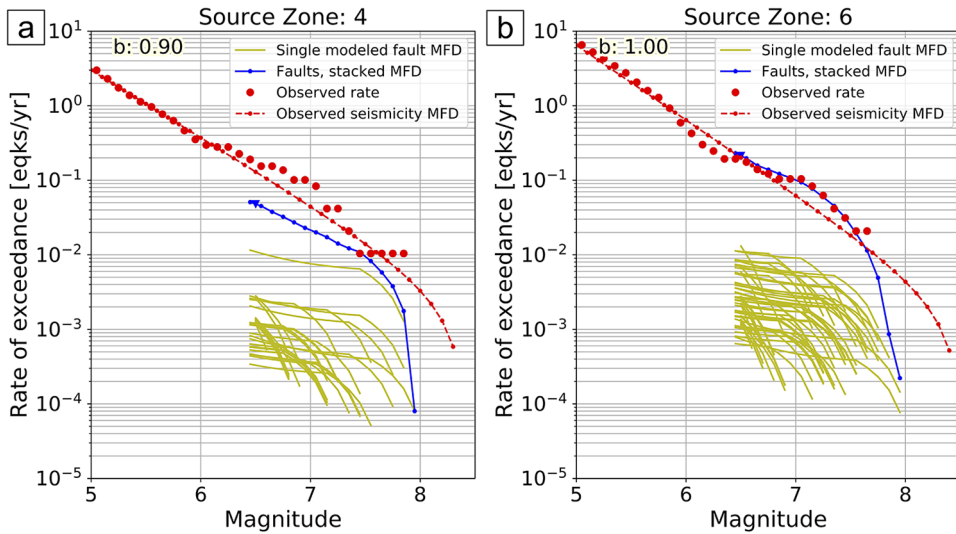
[b]The largest earthquake is pre-1900s.

Figure 4. Example MFDs for (a) source zone 4 and (b) source zone 6—both of which contain faults—showing the degree to which the modeled faults capture the observed seismicity. Each yellow line is the cumulative MFD for a single modeled fault source, and the blue line is the sum of these. The red line and points show the MFD and observed cumulative seismicity rates.

Subduction interface

The subduction interface seismicity is modeled as a set of finite ruptures occurring on a fault surface, where each interface segment corresponds to one fault, and ruptures are floated across the surface and scaled by a magnitude–area scaling relationship. Each

Table 2. Completeness thresholds for each of the tectonic regions

Year	M_w, crustal	M_w interface	M_w slab
1980	5.0	5.0	5.5
1960	6.0	6.0	6.0
1920	7.0	7.0	7.0
1900	8.0	8.0	8.0

interface source has an independent MFD, which, when possible, was derived using a hybrid approach that combines GR statistics from observed seismicity with a characteristic component from tectonics. The Negros and Sulu trenches use only GR MFDs due to data limitations for modeling the characteristic component, but all others use the hybrid approach.

The statistical approach solves for GR *a* and *b* values (a negative exponential) from the declustered sub-catalogs filtered for completeness (Table 2) as in Weichert (1980). The latter approach derives a double-truncated Gaussian distribution to model the maximum magnitude earthquake that an interface segment can theoretically support, that is, a characteristic earthquake. The two approaches are combined into a hybrid model by taking the higher occurrence rate for each magnitude bin, M_w 5.5 to M_{max}.

The magnitude and occurrence rate of the characteristic earthquake for an interface segment are based on the fault area, the convergence rate, and a seismic coupling coefficient. Magnitude was computed from Thingbaijam et al. (2017) magnitude scaling relationships for subduction interfaces. Published convergence rates and seismic coupling coefficients were used to determine the time needed to accumulate enough strain for the characteristic earthquake (Table 3; Galgana et al., 2007; Hsu et al., 2012; Rangin, 2016).

Figure 5 shows an example of the hybrid MFD for the Philippine Trench, segment 1. The characteristic component contributes only a small deflection from the negative exponential GR MFD. Given the low coupling coefficients across most of the subduction zone segments (Table 3), this is the case for all interface segments in the Philippines, and in most cases the characteristic component sits entirely beneath the GR MFD.

Where possible, the resulting MFDs were compared against long term (Holocene to Recent) rates. This is challenging in the Philippines, and mostly limited to the absence of $M_w > 8$ earthquakes impacting Luzon (and thus on the Manila subduction zone) since colonization in 1560 (Hsu et al., 2016). This is consistent with Ramos and Tsutsumi (2010), who conclude that uplift observed on the west coast of Luzon is caused by shallow thrust faults rather than large-magnitude interface events (i.e. large interface events are less likely). The MFDs computed here for the Manila Trench area also consistent, predicting $M_w > 8$ interface earthquake recurrence intervals of almost 1000 years.

Intraslab

Intraslab sources are implemented as a set of ruptures dipping at 45° and 135° within the slab volume of 60 km thickness (the same volume used for tectonic classification). The slab segmentation model (Figure 3b) allows spatial variability in the observed seismicity to be accounted for in the seismic source model while still using non-parametric ruptures. Each slab segment is assigned a single GR MFD (regressed using Weichert, 1980) from

Table 3. Model parameters for subduction sources

Sub. zone	Segment	a	b	$M_{max,obs}$	M_{char}	c (mm/year)	Coupling	N
Manila	1-if	4.083	0.835	7.63[a]	7.89	90[1]	0.01[2]	34
	1-slab[*]	6.658	1.277	6.69[a]				68
	2-if	4.279	0.873	7.24	8.15	60[1]	0.01[2]	33
	2-slab[*]	2.999	0.691	6.85				15
	3-if	6.195	1.108	7.33[a]	8.49	50[1]	0.01[2]	200
	3-slab	5.087	1.050	6.90[a]				9
East Luzon	1-if	3.546	0.770	7.60	8.12	15[2,3]	1.0[2]	20
	2[**]	8.308	1.724	6.40	8.14	9[3]	0.02[2]	17
Philippine	1-if	6.176	1.073	7.52	8.63	30[2,3]	0.27[2]	244
	1-slab	5.344	0.997	8.00[a,b]				31
	2-if	4.689	0.927	7.41[a]	8.04	30[2,3]	0.27[2]	42
	2b-slab	5.118	1.014	7.01				14
Cotabato	1-if	3.318	0.678	8.30[a]	8.08	35[3]	0.41[3]	33
	1-slab	4.081	0.943	6.45				19
Sulu	1-if	3.312	0.797	7.50[a]	N/A	N/A	N/A	7
Negros	1-if	5.127	1.084	6.63[a]	N/A	N/A	N/A	21
Halmahera	1-slab	7.140	1.179	8.01[a]	N/A	N/A	N/A	184
	2-slab	8.219	1.429	7.6	N/A	N/A	N/A	90

Source type is indicated in the segment column. if: interface. slab: intraslab. N: number of earthquakes used to fit the MFD, after completeness filtering and declustering. c: convergence rate.

NA: not applicable.

[a]The largest recorded earthquake was pre-1964 and could have a high magnitude error, or was filtered out using the completeness thresholds and thus not used to compute the MFD.

[b]Manually reassigned.

[1]Hsu et al. (2012), [2]Galgana et al. (2007), and [3]Rangin et al. (2016).

[*]Uses slightly more inclusive completeness (1980, 5.0); [**]East Luzon segment 2 is a transform fault.
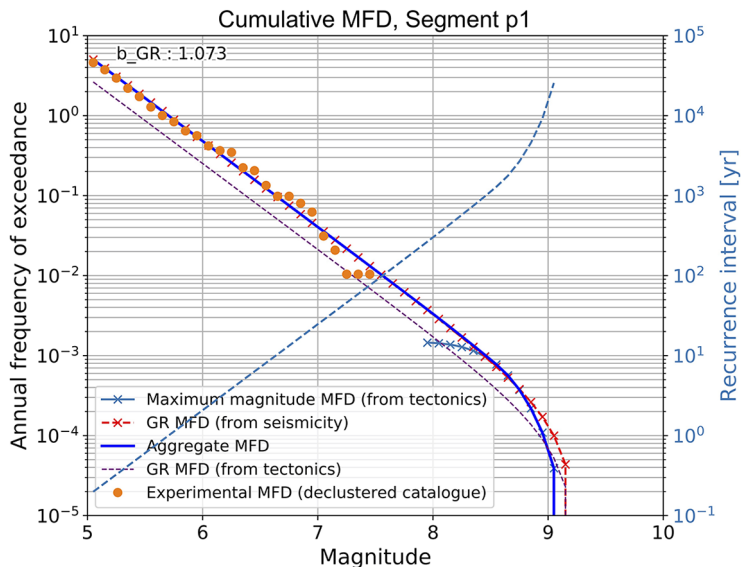

Figure 5. Hybrid MFD for the Philippine trench section 1. The characteristic component only barely deflects the MFD from the Gutenberg–Richter component, as is the case for all interfaces in the PEM.

the declustered sub-catalogs filtered for completeness (Table 2) assuming spatially uniform rates throughout each segment. The MFDs are applied to ruptures of M_w 6.5 to M_{max}, where $M_{max} = M_{max,obs} + 0.5$, using the intraslab magnitude scaling relationship of Strasser (2010; Table 3).

Ground motion characterization

The development of ground motion prediction equations (GMPEs) specific for the Philippines has been limited because of the relatively few strong-motion data available to develop such models. Hence, in recent years, considerable effort has been made to increase the number of strong-motion stations within the Philippines in order to record data of sufficient quality and quantity. In the meantime, GMPEs derived for regions with similar tectonic settings as the Philippines must be applied for national-scale hazard assessments.

The ground motion characterization for the Philippines hazard model is divided into three tectonic regions: active shallow crust, subduction interface, and subduction intraslab, each using a weighted set of GMPEs. Sufficient strong-motion recordings are available for active shallow crustal earthquakes to perform a residual analysis to the GMPEs for some magnitude and distance ranges, while the subduction GMPEs are selected from various global models to account for the full range of possibilities.

Active shallow crust

An evaluation of published GMPEs to crustal earthquakes in the Philippines was originally part of the 2014 PHIVOLCS-Geoscience Australia Risk Analysis for the Philippines project, a hazard and risk analysis for the Greater Metro Manila Area (RAP; Allen et al., 2014). The RAP project performed a residual analysis of ground motion data collected by the Philippine seismic network (PSN) to eight GMPEs, deeming Boore and Atkinson (2008), Chiou and Youngs (2008), Fukushima and Tanaka (1990), and Sadigh et al. (1997) the most suitable for source-to-site distances <60 km. This procedure is described in detail in Supplemental Appendix B.

The GMM (in the form of a logic tree) used in this study is based on the results of the original RAP project assessment. However, the recommended GMPE set is modified to account for more recently published models and choice strategies, and different model utility (e.g. flexible regional hazard model vs city-specific disaster planning). Newer models developed for active shallow crustal and global utility are added to the suite of originally considered GMPEs. For GMPEs derived for several rock quality factors (Q), the low-Q version was selected to account for the more rapid attenuation observed for Philippine earthquakes in the RAP project.

Exclusion criteria based on Bommer et al. (2010) were applied to eliminate GMPEs that do not compute spectral accelerations (SAs), are defined for magnitude types other than M_w, do not cover the magnitude range in the source model, or require parameters that are unavailable and difficult to estimate. These eliminated two of RAP project's original recommendations: Fukushima and Tanaka (1990) and Sadigh et al. (1997).

The final group of candidate GMPEs was as follows: Zhao et al. (2006), Boore and Atkinson (2008), Chiou and Youngs (2008), Abrahamson et al. (2014), Boore et al. (2014; low-Q), Campbell and Bozorgnia (2014; low-Q), Chiou and Youngs (2014), and Bindi et al. (2017).

Residual analysis was not repeated using the new suite of GMPEs. Instead, GMPEs were selected to represent the minimum, maximum, and mean ground motions predicted by the suite of models, capturing the full range of possible values. This accounts for epistemic uncertainty resulting from the limited magnitude–distance pairs available for residual analysis. For example, although the largest-magnitude earthquake considered by the residual analysis was M_w 7.6, the closest source-site distance was >200 km; the next largest earthquake was M_w 6.7. Thus, the amplitudes of ground motions due to large crustal earthquakes in the Philippines are not well-constrained, especially at close distances, and alternative GMPEs cannot be excluded.

The OpenQuake GMPE-SMTK (Strong-Motion Toolkit; Weatherill, 2014) was used to compare amplitude and attenuation patterns among the GMPEs for common rupture types in the source model. For PGA at moderate magnitudes ($\sim M_w$ 6.5), the suite of GMPEs has overall low variation, but as magnitude increases to M_w 8.5—the maximum magnitude allowed by the crustal source model—the predicted values diverge (e.g. Figure 6a).

Boore and Atkinson (2008) and Chiou and Youngs (2008) were selected to account for median ground motion amplitudes from the suite of candidate GMPEs. Both were selected in the RAP residual analysis for their good data model fit with the most common earthquake magnitudes ($M_w \sim$ 5.0–6.7); thus, Chiou and Youngs (2008) is used here despite being superseded by Chiou and Youngs (2014). These were balanced with Zhao et al. (2006), which represents the upper bracket of modeled ground motions, and Boore et al. (2014, low-Q) to reflect the lower bracket of modeled ground motions. Each GMPE is assigned 0.25 weight, allowing the median amplitudes to be somewhat more likely than the extremes.

Subduction

Only a few subduction GMPEs are available for worldwide application. Applying the exclusion principles of Bommer et al. (2010) refines the selection to only four options for both interface and intraslab GMPEs: Youngs et al. (1997), Atkinson and Boore (2003), Zhao et al. (2006), and Abrahamson et al. (2016), and their regional variations. In the absence of records to perform residual analysis, the chosen logic tree captures the range of ground motions spanned by the GMPEs, including a minimum, maximum, and approximate mean estimate, as was done for the crustal GMPEs. Importantly, the selected equations are considered to be representative, and not *true* minima and maxima, as the relative positions of the GMPEs vary among different rupture orientations.

For intraslab earthquakes, the logic tree was selected from trellis plots for the distance range 50–300 km (R_{rup}) and M_w 6.5–8.5, equally weighting (0.33) Zhao et al. (2006), Atkinson and Boore (2003) with the Cascadia term, and Youngs et al. (1997); see Figure 6b. For interface earthquakes, the attenuation patterns of the candidate GMPEs compare differently for different magnitudes, leading to the selection of four equally weighted (0.25) GMPEs: Youngs et al. (1997), Atkinson and Boore (2003), Zhao et al. (2006) with the Cascadia term (e.g. Atkinson and Adams, 2013), and Abrahamson et al. (2016); see Figure 6c. In both tectonic regimes, for short periods, the equation using the Cascadia term usually sits lowest on the trellis plot for PGA; thus, it is included to envelope the lowest possible ground motions, and not to imply that the Philippines and Cascadia have equivalent attenuation patterns.
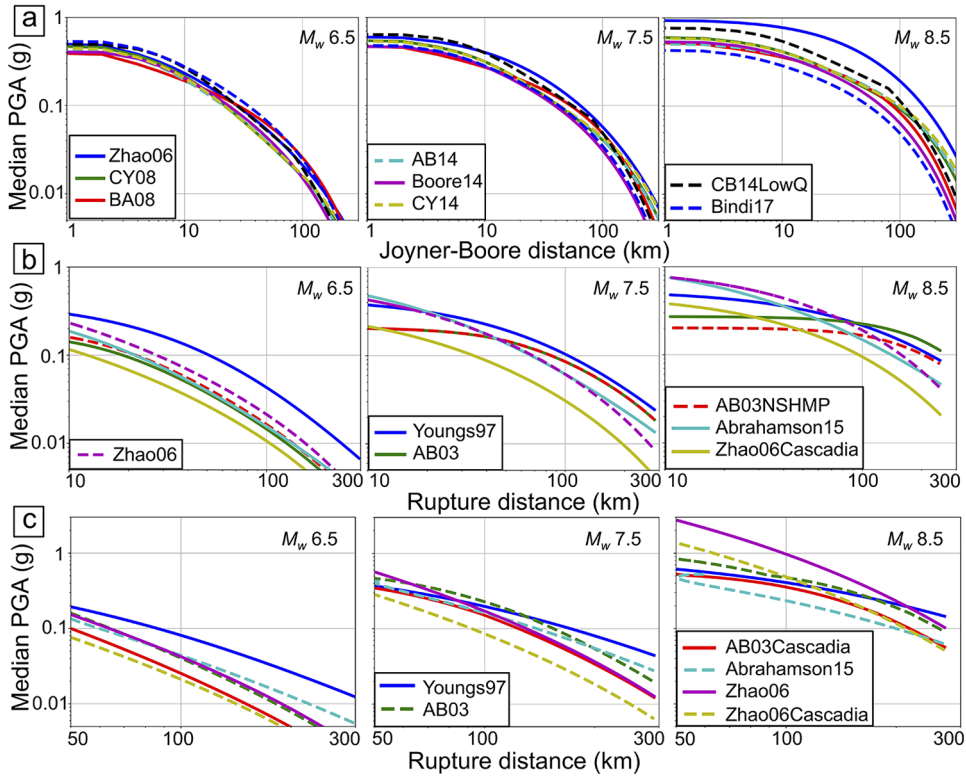
Figure 6. Trellis plots showing median rock site PGA of the GMPEs for (a) active shallow crust, (b) subduction interface, and (c) subduction intraslab for M_w 6.5–8.5 (indicated in upper right corner of each plot). Solid lines are for the selected GMPEs, while dashed lines were only considered. Colors shown in the legends apply to all plots across that tectonic region. The following acronyms all use the standard model of their reference for the respective tectonic region unless otherwise noted. *Zhao06*: Zhao et al. (2006); *CY08*: Chiou and Youngs (2008); *BA08*: Boore and Atkinson (2008); *AB14*: Abrahamson et al. (2014); *Boore14*: Boore et al. (2014); *CY14*: Chiou and Youngs (2014); *CB14LowQ*: Campbell and Bozorgnia (2014), low-*Q* attenuation term; *Bindi17*: Bindi et al. (2017); *Youngs97*: Youngs et al. (1997); *AB03*: Atkinson and Boore (2003); *AB03NSHMP*: Atkinson and Boore (2003), National Seismic Hazard Mapping Program site term; *Abrahamson15*: Abrahamson et al. (2016); *AB03Cascadia*: Atkinson and Boore (2003), Cascadia site term; *Zhao06Cascadia*: Zhao et al. (2006), Cascadia site term.

PSHA results

The OpenQuake engine (Pagani et al., 2014) was used to compute hazard curves at ~3400 sites (~10 km spacing) with reference soil conditions equivalent to V_{S30} of 760–800 m/s for the intensity measures PGA and SA at periods of 0.2, 0.5, 1.0, and 2.0 s. Here, the discussion is limited to PGA for rock sites ($V_{S30} \sim 760$ m/s) for 475 and 2475-year return periods, equivalent to a 10% and 2% probability of exceedance (PoE) in 50 years (Figure 7) for brevity, and because this intensity measure was referenced to determine the seismic coefficient used to calculate the design base shear (Section 208.5.1 and Section 208.5.2) in the latest NSCP. However, the NSCP covers all vertical and horizontal structures nationwide, and so in the upcoming revision, the Association of Structural Engineers of the Philippines (ASEP) will incorporate the full uniform hazard response spectra; for
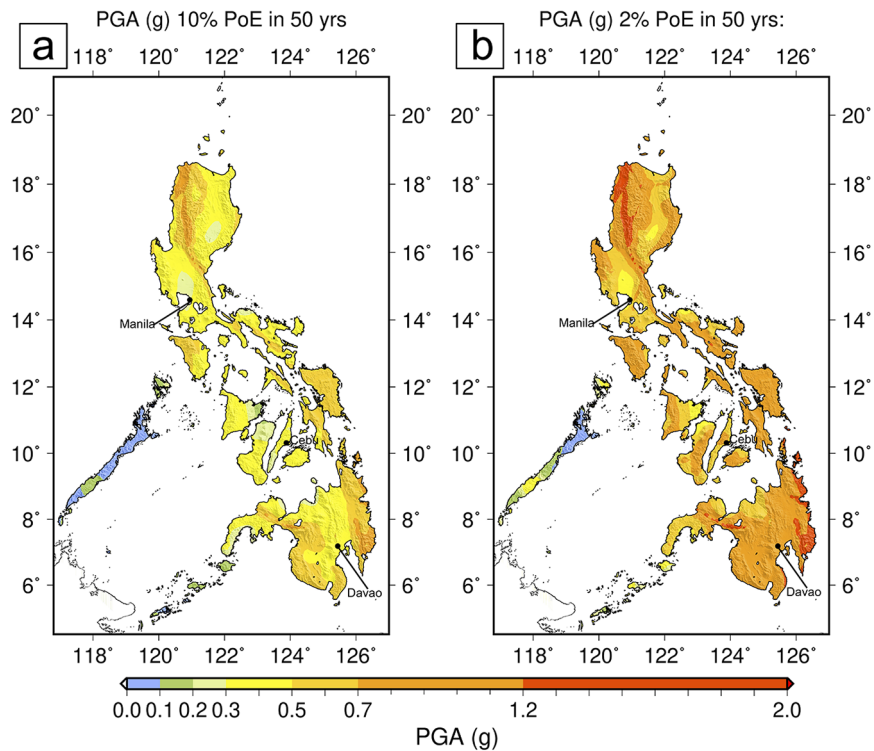
Figure 7. Mean PGA with (a) 10% and (b) 2% PoE in 50 years overlain on the hillshaded SRTM topography (Farr et al., 2007). The same color scale is used for both PoEs. The plotted cities are metropolitan areas evaluated by disaggregation.

this update, seismic design will be based on IBC 2018 (International Code Council (ICC), 2018) and ASCE 7-16 Standard (American Society of Civil Engineers/Structural Engineering Institute (ASCE/SEI), 2013). Supplemental Appendix D discusses results for some additional spectral periods.

The highest PGA hazard occurs in the immediate vicinity of the PFS and other crustal faults, peaking at 1.0*g* and 1.7*g* for 10% and 2% PoE in 50 years, respectively. In the northern Philippines on the island of Luzon, crustal faults with a reverse component lead to wider swaths of high hazard, including >20-km-wide zones with PGA >0.6*g* for 10% PoE in 50 years, whereas along strike-slip faults, these peak values are confined to narrow bands about the fault traces. The contribution of subduction interfaces to PGA is less apparent, but distinguishable along some coast lines, such as the eastern coast of Davao near the Philippine Trench, where hazard isolines are parallel to and increasing toward the shoreline. In this region, the PGA maxima are less widespread or pronounced, but the local distributed seismicity rates and highly productive slabs cause higher background (off-fault) hazard than in the north.
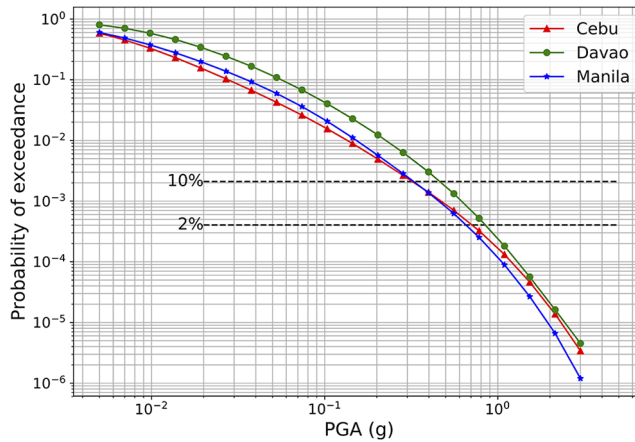
Figure 8. Hazard curves for the three metropolitan areas in the Philippines. PoE is for an investigation period of 1 year. Dashed black lines are at 0.000404 and 0.002105, corresponding to 2% and 10% PoE in 50 years.

Discussion

Comparison with previous hazard models

Both the 2017 PEM seismic hazard model and the one presented here demonstrate an increased understanding of seismic sources in the Philippines compared to 1994, when the Thenhaus et al. (1994) model was published. For 10% PoE in 50 years on rock site, the Thenhaus et al. (1994) model yielded median PGA values of <0.3*g* for the whole archipelago; the values from the new models are higher almost everywhere (>0.3*g* on most of the archipelago), and the spatial resolution of the newly produced hazard maps is improved. In particular, the bands of concentrated and heightened shaking hazard surrounding crustal faults in the new model are absent from the 1994 model, which did not include shallow crustal fault sources.

Comparing the model presented here to the 2017 PEM (Peñarubia et al., 2017) for rock site median PGA with 10% PoE in 50 years, contour patterns are similar in many locations, as many of the same source geometries were used. Near faults, the model presented here predicts higher values of PGA, partly because in the PEM model, PGA values were truncated for structural design considerations. A second reason is that different methodologies were used to constrain fault activity rates: the PEM model used nearby historical and instrumental occurrences, while the present model uses slip rates. The impact of intraslab seismicity, which was not included in the original PEM model, is also noticeable; in some key areas (e.g. in the south near Davao), the off-fault hazard is elevated in the newest model, with the background PGA increasing by ∼0.1*g*. Spatially variable hazard away from faults is also attributable to the use of smoothed seismicity to model background sources, as opposed to constant-rate area sources used in the PEM model.

Figure 8 shows the hazard curves for mean PGA for the most populated Philippine metropolitan areas: Metro Manila, Metro Davao, and Metro Cebu. In Metro Davao, the hazard is highest, with 10% PoE of ∼0.5*g* in 50 years and 2% PoE of ∼0.8*g*. In Metro Manila and Metro Cebu, PGA with 10% PoE in 50 years is ∼0.3*g*, and 2% PoE in 50 years is 0.6–0.7*g*.
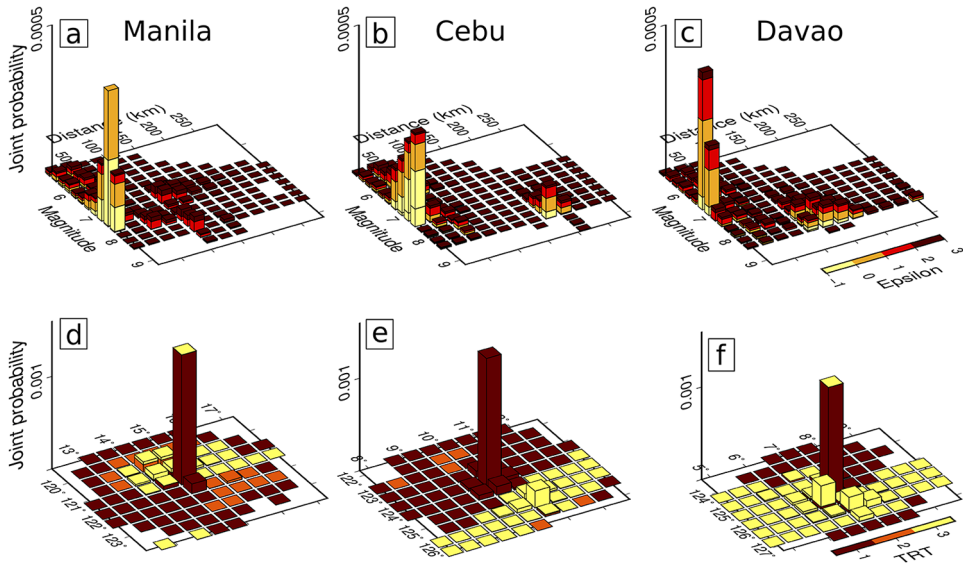
Figure 9. Disaggregation results for mean PGA with a 10% PoE in 50 years for three metropolitan areas in the Philippines: (a, d) Manila (121.038°E, 14.622°N), (b, e) Cebu (123.830°E, 10.298°N), and (c, f) Davao (125.427°E, 7.203°E). (a, b, c) Disaggregation is by magnitude and distance, colored by epsilon: the number of standard deviations from the mean of a GMPE. In all cases, the dominating contributors to hazard are earthquakes with hypocenters <25 km from the metro area, and M_w ~ 7.0. Earthquakes of other distance–magnitude combinations make much lower contributions to the mean PGA. (d, e, f) Disaggregation is by latitude, longitude, and tectonic region, with plots centered on their relevant cities. Color indicates source tectonic region type (1: active shallow crust, 2: interface, and 3: intraslab). Hazard is dominated by active shallow crustal sources very close to the metropolitan area.

Disaggregation

Seismic source disaggregation (e.g. Bazzurro and Cornell, 1999; Pagani and Marcellini, 2007) was used to further understand the ground-shaking hazard in these metropolitan areas, revealing which sources contribute most to the hazard at each location. The disaggregation indicates the contributions to a given value of hazard provided by discrete combinations of fundamental parameters used in the hazard integral, such as magnitude, distance, and epsilon. Figure 9 shows the results for Metro Manila, Metro Davao, and Metro Cebu, focusing on PGA with a 10% PoE in 50 years on site class $V_{S30} = 760$ m/s; the following discussion refers to this intensity measure and return period. Sources with a PoE $>1.0e-20$ and within the model integration distance (300 km) were included.

In Metro Manila, the capital city and largest metropolitan area in the Philippines, the mean PGA is 0.32g. Figure 9a shows source contribution at magnitude–distance combinations binned by M_w 0.25 and 25 km. The largest sources of hazard contribution are close by, and especially those within 25 km with M_w ~ 6.50–7.75. At ~100–150 km distance, earthquakes approaching M_w 8.0 form a second cluster of non-zero probabilities. Figure 9d shows the hazard contributions in mapview, differentiated in color by tectonic region type. The hazard is dominated by active shallow crustal faulting close to or within the metropolitan area. In particular, the West Valley Fault (Rimando and Knuepfer, 2006), which slips at >5 mm/year, manifests through the eastern part of the city. The second highest

contributor is the Manila subduction zone to the west, where both interface and intraslab earthquakes can produce PGA values in Manila of >0.32*g*, accounting for some of the largest magnitudes in Figure 9a. These distant sources, which also include interface earthquakes on the Philippine Trench, though less likely, may cause strong ground shaking in Metro Manila.

Metro Cebu is in the central part of the archipelago on the island of Cebu and has a mean PGA of 0.32*g*. Figure 9b shows that similar to Metro Manila, most occurrences of this PGA value are due to nearby earthquakes (<75 km source-to-site distance, and especially <25 km source-to-site) with the highest contributions from earthquakes of M_w 6.5–7.5. At ~200 km distance, large earthquakes ($M_w > 7$) also have non-zero probabilities. Most other distance–magnitude combinations have near-negligible PoEs. Figure 9e shows that the near-site sources are again active shallow crust, as the metropolitan area is situated in a compressional region, among several faults. To the east, the disaggregation shows the contribution of earthquakes within the downgoing slab of the Philippine subduction zone. For this PoE, and for high-frequency PGA, the Negros and Philippine subduction interfaces have low contributions.

Metro Davao, in the far south of the Philippines, has a mean PGA of 0.45*g*. Figure 9c shows that like the other metro areas, the earthquakes occurring <75 km from the reference point of disaggregation have the most probable impact, with the highest PoEs attributed to M_w 6.5–7.0 events within 25 km of the site. There is additional hazard contribution from farther away earthquake sources ($M_w \sim$ 7.0–8.5 km, 100–200 km source-to-site distances). Figure 9f shows that the near-site sources are mostly active shallow crust, as Davao sits atop a group of short sinistral and sinistral-reverse faults which collectively slip at >5 mm/year. To the south and east, the disaggregation shows the effect of the Halmahera and Philippine slabs, where large earthquakes are likely to occur in the next 500 years and contribute more hazard than the interface sources.

Model uncertainty

The hazard model presented here aims to account for all potential earthquake sources that threaten the Philippines. However, some epistemic uncertainty is currently unaccounted for. The ground motion logic tree uses branches for each tectonic region type to consider all possible ground motions for all modeled earthquakes, including those that have not occurred during the instrumental period and have distance–magnitude pairs that have not been recorded. As more strong-motion data become available, the GMPEs selection will be better constrained, and Philippine-specific GMMs may be developed.

In contrast, epistemic uncertainty in the source model remains unaccounted for—an aspect of the model that should be improved in future efforts. For example, the current model employs a single MFD and single M_{max} for each source. M_{max} is determined by either adding a delta value to the magnitude of the largest observed earthquake or derived using a magnitude scaling relationship; however, only one delta value and a single rupture configuration are considered. This is in contrast to recent earthquakes, such as the 2010 M_w 7.2 El Mayor Cucapah earthquake (e.g. Fletcher et al., 2014) and the 2016 M_w 7.8 Kaikōura earthquake (e.g. Hamling et al., 2017), which have ruptured surprising combinations of faults, producing larger magnitudes than if the ruptures had confined to single faults. Similarly, the subduction segmentation model considers only one branch, within which the Philippine and Manila trenches are not expected to rupture their entire lengths in a single earthquake. A source model allowing multi-segment ruptures would reallocate
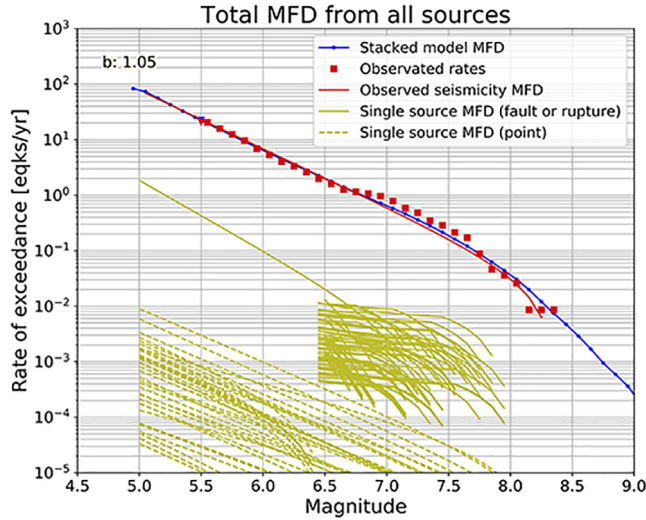
Figure 10. Total MFD computed by summing the occurrence rates for all sources in the source model. Each yellow line is the MFD for a single source. There are ~15,000 point sources, but only a few are shown for clarity. The blue line is the sum of these lines. Red squares are observed rates of exceedance by 0.1 magnitude bin. The solid red line is the MFD fit to these points, with the listed *b* value.

some moment release from the current maximum magnitude earthquakes to even higher magnitude, less frequent occurrences; this would likely lower the hazard for return periods investigated here, while raising hazard at very long return periods. Because the model presented herein has regional coverage, and the intended use is for typical buildings, infrastructure, and certain critical facilities (e.g. schools and hospitals), we do not include multi-segment rupture configurations on the Philippine and Manila trenches. However, in future versions of the PSHA model, the sensitivity of the hazard results to these issues may be tested and included in the logic tree.

As an initial test of the model, seismicity rates produced by all sources in the source model are compared to the observed seismicity (Figure 10). The MFDs for all sources are summed to produce a single model MFD, and the rates of exceedance for each magnitude are compared to the observed seismicity (filtered by completeness and declustered, as in the catalog preprocessing) and its computed MFD. The two MFDs match reasonably well, with slight underpredictions of seismicity for M_w 6.9–M_w 7.7. A possible explanation is that the segmentation definitions for continuous or semi-continuous fault traces with similar or identical characterizations, for example, the main strand of the PFS, may be inaccurate. The direct effect of fault segmentation is a higher number of more evident faults with lower M_{max}, and more frequent earthquakes at M_w 6.5. In other words, the seismic moment is allocated more to lower magnitudes than if the faults were modeled as a single source. In addition, the crustal faulting away from the PFS includes many short faults with poorly constrained slip rates. The contribution from these MFDs is concentrated at $M_w < 7.0$.

Model and data MFD mismatches for magnitudes $M_w > 6.5$ are familiar from the UCERF 2 model (Field et al., 2009) and typically manifest as a "bulge" in modeled seismicity compared to the observed rates (see Supplemental Appendix E). The UCERF 3 model (Field et al., 2014) accounted for the discrepancy by relaxing fault segmentation, thus distributing more seismic moment to larger magnitude occurrences. Here, the use of

combined fault segments and Youngs and Coppersmith (1985) MFDs for larger sources corrects for this; however, future PSHA models for the Philippine archipelago should further investigate the criteria for selecting among MFD types, and rupture of multiple faults together, accounting for El Mayor Cucapah- and Kaikōura-type events (Fletcher et al., 2014; Hamling et al., 2017).

Conclusion

The PSHA model for the Philippines presented here is an update and recalculation of the 1994 and 2017 models (PHIVOLCS, 2017; Peñarubia et al., 2017; Thenhaus et al., 1994), using modern modeling approaches, updated seismicity, and significantly improved consideration of the contributing sources.

Although the reported mean PGA (with 10% PoE in 50 years) in all three metropolitan areas explored herein is dominated by nearby active crustal faulting, it is important to note that the hazard due to subduction earthquakes (both interface and intraslab) is non-zero (e.g. Figure 9), and that hazard contribution of large magnitude events from these sources becomes significant closer to some trenches and at longer spectral periods ($T > 1$ s) to high-rise buildings and long-span structures due to resonance effect. In addition, although the shaking caused by subduction earthquakes may produce lower PGA than that by closeby crustal faulting, interface sources may also contribute to higher tsunami hazard.

The hazard maps and model presented here may be used to enhance appropriate and site-specific seismic design capacity of future engineered structures and related facilities and encourage retrofit of existing ones in hopes to improve building resilience and safety of occupants to future intense earthquakes, considering acceptable risks and engineering economy. However, it is crucial to emphasize that the resulting PGA values do not directly substitute into the base shear derivation and the maps and information presented here should be treated with prudence and not as a design threshold.

ORCID iD

Trevor I Allen https://orcid.org/0000-0003-3420-547X

Supplemental material

Supplemental material for this article is available online.

References

Abrahamson NA, Gregor N and Addo K (2016) BC Hydro ground motion prediction equations for subduction earthquakes. *Earthquake Spectra* 32(1): 23–44.

Abrahamson NA, Silva WJ and Kamai R (2014) Summary of the ASK14 ground motion relation for active crustal regions. *Earthquake Spectra* 30(3): 1025–1055.

Akkar S and Bommer JJ (2010) Empirical equations for the prediction of PGA, PGV, and spectral accelerations in Europe, the Mediterranean region, and the Middle East. *Seismological Research Letters* 81(2): 195–206.

Allen TI, Ryu H, Bautista B, Bautista ML, Narag I, Sevilla WI, Melosantos MLP, Papiona K and Bonita J (2014) *Enhancing Risk Analysis Capacities for Flood, Tropical Cyclone Severe Wind and Earthquake for the Greater Metro Manila Area* (Component 5). Canberra, ACT, Australia: Geoscience Australia.

Ambraseys NN, Douglas J, Sarma SK and Smit PM (2005) Equations for the estimation of strong ground motions from shallow crustal earthquakes using data from Europe and the Middle East: Horizontal peak ground acceleration and spectral acceleration. *Bulletin of Earthquake Engineering* 3(1): 1–53.

American Society of Civil Engineers/Structural Engineering Institute (ASCE/SEI) (2013) *Minimum Design Loads and Associated Criteria for Buildings and Other Structures* (ASCE/SEI 7-16). Reston, VA: ASCE.

Atkinson GM and Adams J (2013) Ground motion prediction equations for application to the 2015 Canadian national seismic hazard maps. *Canadian Journal of Civil Engineering* 40: 988–998.

Atkinson GM and Boore DM (2003) Empirical ground-motion relations for subduction-zone earthquakes and their application to Cascadia and other regions. *Bulletin of the Seismological Society of America* 93(4): 1703–1729.

Aurelio MA (2000) Shear partitioning in the Philippines: Constraints from Philippine fault and global positioning system data. *Island Arc* 9(4): 584–597.

Bacolcol TC (2003) *Etude geodesique de la faille Philippine dans les Visayas*. Unpublished Doctoral Dissertation, Universite Pierre et Marie Curie, Paris.

Bacolcol TC, Barrier E, Duquesnoy T, Aguilar A, Jorgio R, de la, Cruz R and Lasala M (2005) GPS constraints on Philippine fault slip rate in Masbate Island, central Philippines. *Journal of the Geological Society of the Philippines* 60: 1–7.

Bacolcol TC, Sapla G, Pelicano A, Luis A Jr, Jorgio R, Marfito B, Paras M, Ragadio Z, Baloto A and Absin O (2017) *Interseismic velocities and GPS motions associated with 6 July 2017 M6.5 Philippine fault (Leyte Segment) earthquake*. PHIVOLCS open-file report no. 18–02, 10 pp. Quezon City, Philippines: Philippine Institute of Volcanology and Seismology.

Barrier E, Huchon P and Aurelio M (1991) Philippine fault: A key for Philippine kinematics. *Geology* 19: 32–35.

Bautista MLP and Oike K (2000) Estimation of the magnitudes and epicenters of Philippine historical earthquakes. *Tectonophysics* 317: 137–169.

Besana GM and Ando M (2005) The central Philippine Fault Zone: Location of great earthquakes, slow events and creep activity. *Earth Planets and Space* 57(10): 987–994.

Bindi D, Cotton F, Kotha SR, Bosse C, Stromeyer D and Grünthal G (2017) Application-driven ground motion prediction equation for seismic hazard assessments in non-cratonic moderate-seismicity areas. *Journal of Seismology* 21(5): 1201–1218.

Boore DM and Atkinson GM (2008) Ground-motion prediction equations for the average horizontal component of PGA, PGV, and 5%-damped PSA at spectral periods between 0.01 s and 10.0 s. *Earthquake Spectra* 24(1): 99–138.

Boore DM, Stewart JP, Seyhan E and Atkinson GM (2014) NGA-West2 equations for predicting PGA, PGV, and 5% damped PSA for shallow crustal earthquakes. *Earthquake Spectra* 30(3): 1057–1085.

Campbell KW and Bozorgnia Y (2014) NGA-West2 ground motion model for the average horizontal components of PGA, PGV, and 5% damped linear acceleration response spectra. *Earthquake Spectra* 30(3): 1087–1115.

Chiou BSJ and Youngs RR (2008) An NGA model for the average horizontal component of peak ground motion and response spectra. *Earthquake Spectra* 24(1): 173–215.

Chiou BSJ and Youngs RR (2014) Update of the Chiou and Youngs NGA model for the average horizontal component of peak ground motion and response spectra. *Earthquake Spectra* 30(3): 1117–1153.

Daligdig JA (1997) *Recent faulting and paleoseismicity along the Philippine fault zone, north central Luzon, Philippines.* Unpublished Doctoral Dissertation, Kyoto University, Kyoto, Japan, 73 pp.

Dziewonski AM, Chou TA and Woodhouse JH (1981) Determination of earthquake source parameters from waveform data for studies of global and regional seismicity. *Journal of Geophysical Research: Solid Earth* 86: 2825–2852.

Ekström G, Nettles M and Dziewonski AM (2012) The global CMT project 2004–2010: Centroid-moment tensors for 13,017 earthquakes. *Physics of the Earth and Planetary Interiors* 200–201: 1–9.

Farr TG, Rosen PA, Caro E, Crippen R, Duren R, Hensley S, Kobrick M, Paller M, Rodriguez E, Roth L, Seal D, Shaffer S, Shimada J, Umland J, Werner M, Oskin M, Burbank D and Alsdorf D (2007) The shuttle radar topography mission. *Reviews of Geophysics* 45(2): RG2004.

Field EH, Arrowsmith RJ, Biasi GP, Bird P, Dawson TE, Felzer KR, Jackson DD, Johnson KM, Jordan TH, Madden C, Michael AJ, Milner KR, Page MT, Parsons T, Powers PM, Shaw BE, Thatcher WR, Weldon RJ and Zeng Y (2014) Uniform California earthquake rupture forecast, version 3 (UCERF3)—the time-independent model. *Bulletin of the Seismological Society of America* 104: 1122–1180.

Field EH, Dawson TE, Felzer KR, Frankel AD, Gupta V, Jordan TH, Parsons T, Petersen MD, Stein RS, Weldon RJ and Wills CJ (2009) Uniform California earthquake rupture forecast, version 2 (UCERF 2). *Bulletin of the Seismological Society of America* 99: 2053–2107.

Fitch TJ (1972) Plate convergence, transcurrent faults, and internal deformation adjacent to Southeast Asia and the western Pacific. *Journal of Geophysical Research* 77(23): 4432–4460.

Fletcher JM, Teran OJ, Rockwell TK, Oskin ME, Hudnut KW, Mueller KJ, Spelz RM, Akciz SO, Masana E, Faneros G, Fielding EJ, Leprince S, Morelan AE, Stock J, Lynch DK, Elliott AJ, Gold P, Liu-Zeng J, González-Ortega A, Hinojosa-Corona A and González-García J (2014) Assembly of a large earthquake from a complex fault system: Surface rupture kinematics of the 4 April 2010 El Mayor–Cucapah (Mexico) M_w 7.2 earthquake. *Geosphere* 10(4): 797–827.

Frankel A (1995) Mapping seismic hazard in the central and eastern United States. *Seismological Research Letters* 66(4): 8–21.

Fukushima Y and Tanaka T (1990) A new attenuation relation for peak horizontal acceleration of strong earthquake ground motion in Japan. *Bulletin of the Seismological Society of America* 80(4): 757–783.

Galgana G, Hamburger M, McCaffrey R, Corpuz E and Chen Q (2007) Analysis of crustal deformation in Luzon, Philippines using geodetic observations and earthquake focal mechanisms. *Tectonophysics* 432(1–4): 63–87.

Garcia CL, Valenzuela R, Arnold EP, Macalinag TG, Ambubuyog GF, Lance NT, Cordeta JD, Doniego AG, Dabi AC, Balce GR and Su FS (1985) Series on Seismology: Philippines. In: *Southeast Asia Association of Seismology and Earthquake Engineering*, vol. 4, pp. 743–792. US Geological Survey-USAID Singapore.

Gardner JK and Knopoff L (1974) Is the sequence of earthquakes in Southern California, with aftershocks removed, Poissonian? *Bulletin of the Seismological Society of America* 64(5): 1363–1367.

General Bathymetric Chart of the Oceans (GEBCO) (2008) *The GEBCO_08 Grid.* International Hydrographic Organization and the Intergovernmental Oceanographic Commission of UNESCO, p. 19. Available at: http://www.gebco.net/

Gutenberg B and Richter CF (1944) Frequency of earthquakes in California. *Bulletin of the Seismological Society of America* 34: 185–188.

Hamling IJ, Hreinsdóttir S, Clark K, Elliott J, Liang C, Fielding E, Litchfield N, Villamor P, Wallace L, Wright TJ, D'Anastasio E, Bannister S, Burbidge D, Denys P, Gentle P, Howarth J, Mueller C, Palmer N, Pearson C, Power W, Barnes P, Barrell DJ, Van Dissen R, Langridge R, Little T, Nicol A, Pettinga J, Rowland J and Stirling M (2017) Complex multifault rupture during the 2016 M_w 7.8 Kaikōura earthquake, New Zealand. *Science* 356(6334): eaam7194.

Hayes GP, Moore GL, Portner DE, Hearne M, Flamme H, Furtney M and Smoczyk GM (2018) Slab2, a comprehensive subduction zone geometry model. *Science* 362(6410): 58–61.

Hsu YJ, Yu SB, Loveless JP, Bacolcol T, Solidum R, Luis A Jr, Pelicano A and Woessner J (2016) Interseismic deformation and moment deficit along the Manila subduction zone and the Philippine Fault system. *Journal of Geophysical Research: Solid Earth* 121(10): 7639–7665.

Hsu YJ, Yu SB, Song TRA and Bacolcol T (2012) Plate coupling along the Manila subduction zone between Taiwan and northern Luzon. *Journal of Asian Earth Sciences* 51: 98–108.

International Code Council (ICC) (2018) *International Residential Code.* Country Club Hills, IL: ICC.

Kanno T, Narita A, Morikawa N, Fujiwara H and Fukushima Y (2006) A new attenuation relation for strong ground motion in Japan based on recorded data. *Bulletin of the Seismological Society of America* 96(3): 879–897.

Kaverina AN, Lander AV and Prozorov AG (1996) Global creepex distribution and its relation to earthquake-source geometry and tectonic origin. *Geophysical Journal International* 125(1): 249–265.

Laske G, Masters GT, Ma Z and Pasyanos M (2013) *Update on CRUST1.0—A 1-Degree Global Model of Earth's Crust*, vol. 15 (Geophysical research abstracts). Vienna: EGU General Assembly.

Leonard M (2010) Earthquake fault scaling: Self-consistent relating of rupture length, width, average displacement, and moment release. *Bulletin of the Seismological Society of America* 100(5A): 1971–1988.

Molas GL and Yamazaki F (1994) Seismic macrozonation of the Philippines based on seismic hazard analysis. *Journal of Structural Mechanics and Earthquake Engineering* 11: 33s–43s.

National Structural Code of the Philippines (NSCP) (2015) *NSCP C101-15*, vol. 1. 7th ed. Manila, Philippines: Association of Structural Engineers of the Philippines (ASEP).

Pagani MM and Marcellini A (2007) Seismic-hazard disaggregation: A fully probabilistic methodology. *Bulletin of the Seismological Society of America* 97(5): 1688–1701.

Pagani MM, Monelli D, Weatherill G, Danciu L, Crowley H, Silva V, Henshaw P, Butler L, Nastasi M, Panzeri L, Simionato M and Vigano D (2014) OpenQuake engine: An open hazard (and risk) software for the Global Earthquake Model. *Seismological Research Letters* 85(3): 692–702.

Papiona KL and Kinugasa Y (2008) Trenching surveys along the Masbate segment of the Philippine fault zone. *Journal of the Geological Society of the Philippines* 64: 19–53.

Pasyanos ME, Masters GT, Laske G and Ma Z (2014) LITHO1.0: An updated crust and lithospheric model of the Earth. *Journal of Geophysical Research: Solid Earth* 119(3): 2153–2173.

Peñarubia HC (2017) Seismic coefficient exceedance in the recent destructive earthquake events in the Philippines. In: *Proceedings of the 18th Association of Structural Engineers of the Philippines (ASEP) international convention*, Quezon City, Philippines, 25–27 May.

Peñarubia HC, Grutas RN and Deocampo JB (2017) Probabilistic seismic hazard analysis of the Philippines. In: *Proceedings of the 18th Association of Structural Engineers of the Philippines (ASEP) international convention*, Quezon City, Philippines, 25–27 May.

Perez JS and Tsutsumi H (2011) Paleoseismic studies along the Philippine fault zone, eastern Mindanao, Philippines. In: *Proceedings of the symposium on Japan Geoscience Union meeting*, Chiba, Japan, 22–27 May.

Perez JS and Tsutsumi H (2017) Tectonic geomorphology and paleoseismology of the Surigao segment of the Philippine fault in northeastern Mindanao Island, Philippines. *Tectonophysics* 699: 244–257.

Perez JS, Tsutsumi H, Cahulogan MT, Cabanlit DP, Abigania MIT and Nakata T (2015) Fault distribution, segmentation and earthquake generation potential of the Philippine fault in eastern Mindanao, Philippines. *Journal of Disaster Research* 10(1): 74–82.

Philippine Institute of Volcanology and Seismology (PHIVOLCS) (2017) *The Philippine Earthquake Model: A Probabilistic Seismic Hazard Assessment of the Philippines and of Metro Manila*. Available at: https://www.phivolcs.dost.gov.ph/images/PEM.pdf

Pubellier M, Bader AG, Rangin C, Deffontaines B and Quebral R (1999) Upper plate deformation induced by subduction of a volcanic arc: The Snellius Plateau (Molucca Sea, Indonesia and Mindanao, Philippines). *Tectonophysics* 304(4): 345–368.

Rangin C (2016) Rigid and non-rigid micro-plates: Philippines and Myanmar-Andaman case studies. *Comptes Rendus Geoscience* 348(1): 33–41.

Rangin C, Le Pichon X, Mazzotti S, Pubellier M, Chamot-Rooke N, Aurelio M, Walpersdorf A and Quebral R (1999) Plate convergence measured by GPS across the Sundaland/Philippine sea plate deformed boundary: The Philippines and eastern Indonesia. *Geophysical Journal International* 139(2): 296–316.

Rong Y, Pagani MM, Magistrale H and Weatherill G (2017) Modeling seismic hazard by integrating historical earthquake, fault, and strain rate data. In: *Proceedings of the 16th world conference on earthquake engineering*, Santiago, 9–13 January, paper no. 448.

Sadigh K, Chang CY, Egan JA, Makdisi F and Youngs RR (1997) Attenuation relationships for shallow crustal earthquakes based on California strong motion data. *Seismological Research Letters* 68(1): 180–189.

Stiphout T, Van Zhuang J and Marsan D (2012) Theme V—models and techniques for analysing seismicity. Technical report, Community Online Resource for Statistical Seismicity Analysis, p. 22. Available at: http://www.corssa.org

Su SS (1988) Seismic hazard analysis for the Philippines. *Natural Hazards* 1: 27–44.

Thenhaus PC, Hanson SL, Algermissen ST, Bautista BC, Bautista ML, Punongbayan BJ and Punongbayan RS (1994) *Estimates of the Regional Ground Motion Hazard of the Philippines*. National Disaster Mitigation of the Philippines, pp. 45–60.

Thingbaijam KKS, Mai PM and Goda K (2017) New empirical earthquake source-scaling laws. *Bulletin of the Seismological Society of America* 107(5): 2225–2246.

Torregosa RF, Sugito M and Nojima N (2002) Assessment of seismic hazard and microzoning in the Philippines. *Journal of Structural Mechanics and Earthquake Engineering* 19(2): 81s–98s.

Tsutsumi H and Perez JS (2013) Large-scale digital mapping of the Philippine fault zone based on aerial photograph interpretation. *Active Faults Research* 39: 29–37.

Tsutsumi H, Daligdig JA, Goto H, Tungol NM, Kondo H, Nakata T, Okuno M and Sugito N (2006) Timing of surface-rupturing earthquakes on the Philippine fault zone in Central Luzon Island, Philippines. *EOS Transactions American Geophysical Union* 87: 52.

Tsutsumi H, Perez JS, Marjes JU, Papiona KL and Ramos NT (2015) Coseismic displacement and recurrence interval of the 1973 Ragay Gulf earthquake, southern Luzon, Philippines. *Journal of Disaster Research* 10(1): 83–90.

Turcotte DL and Schubert G (2014) *Geodynamics*. Cambridge: Cambridge University Press, 636 pp.

Uhrhammer RA (1985) Seismicity record, M> 2.5, for the central. Clement F Shearer, p. 199

Weatherill GA (2014) *Openquake Ground Motion Toolkit—User Guide* (Technical report). Pavia: Global Earthquake Model (GEM) Foundation.

Weatherill GA, Pagani MM and Garcia J (2016) Exploring earthquake databases for the creation of magnitude-homogeneous catalogues: Tools for application on a regional and global scale. *Geophysical Journal International* 206(3): 1652–1676.

Weichert DH (1980) Estimation of the earthquake recurrence parameters for unequal observation periods for different magnitudes. *Bulletin of the Seismological Society of America* 70(4): 1337–1346.

Wells DL and Coppersmith KJ (1994) New empirical relationships among magnitude, rupture length, rupture width, rupture area, and surface displacement. *Bulletin of the Seismological Society of America* 84(4): 974–1002.

Wessel P, Smith WHF, Scharroo R, Luis J and Wobbe F (2013) Generic mapping tools: Improved version released. *Eos Transactions American Geophysical Union* 94: 409–410.

Youngs RR and Coppersmith KJ (1985) Implications of fault slip rates and earthquake recurrence models to probabilistic seismic hazard estimates. *Bulletin of the Seismological Society of America* 75: 939–964.

Youngs RR, Chiou SJ, Silva WJ and Humphrey JR (1997) Strong ground motion attenuation relationships for subduction zone earthquakes. *Seismological Research Letters* 68(1): 58–73.

Yu S-B, Kuo L-C, Punongbayan RS and Ramos EG (1999) GPS observation of crustal deformation in the Taiwan-Luzon region. *Geophysical Research Letters* 26(7): 923–926.

Yumul GP, Dimalanta CB and Tamayo RA (2005) Indenter-tectonics in the Philippines: Example from the Palawan microcontinental block—Philippine mobile belt collision. *Resource Geology* 55(3): 189–198.

Yumul GP Jr, Dimalanta CB, Tamayo RA Jr and Maury RC (2003) Collision, subduction and accretion events in the Philippines: A synthesis. *Island Arc* 12(2): 77–91.

Zhang Q, Guo F, Zhao L and Wu Y (2017) Geodynamics of divergent double subduction: 3-D numerical modeling of a Cenozoic example in the Molucca Sea region, Indonesia. *Journal of Geophysical Research: Solid Earth* 122(5): 3977–3998.

Zhao JX, Zhou S, Zhou J, Zhao C, Zhang H, Zhang Y, Gao P, Lan X, Rhoades D, Fukushima Y, Somerville PG and Irikura K (2016) Ground-motion prediction equations for shallow crustal and upper-mantle earthquakes in Japan using site class and simple geometric attenuation functions. *Bulletin of the Seismological Society of America* 106(4): 1552–1569.